Tunable strong coupling between a transmon and a magnon

Feng-Yang Zhang [1,*] Shi-Wen He,[2] Tong Liu [3] Qi-Cheng Wu,[3] and Chui-Ping Yang[4,†]
[1]*School of Physics and Materials Engineering, Dalian Minzu University, Dalian 116600, China*
[2]*School of Physics, Dalian University of Technology, Dalian 116024, China*
[3]*Quantum Information Research Center, Shangrao Normal University, Shangrao 334001, China*
[4]*Department of Physics, Hangzhou Normal University, Hangzhou 310036, China*

(Received 23 March 2023; accepted 8 February 2024; published 29 February 2024)

Coherent coupling between a ferromagnetic magnon and a superconducting qubit demonstrates a special fascination in the quantum information field. Here, we construct a hybrid system to realize tunable strong coupling between a transmon and a magnon. In a hybrid system, the transmon couples to a cavity while the magnon couples to the other cavity. Meanwhile, the two cavities are coupled via a hopping interaction. In addition, we demonstrate some applications of this system to quantum information. Specifically, a high-fidelity $i\text{SWAP}^{\dagger}$ gate and a maximally entangled state between the transmon and the magnon with this coupling system can be realized even if the dissipation is considered. Moreover, by employing more cavities and magnons, the W-type entangled state can be created with multiple transmons. This hybrid system provides an alternative platform for scalable quantum information processing.

DOI: 10.1103/PhysRevA.109.022442

I. INTRODUCTION

Hybrid quantum systems provide an elegant platform for quantum information processing, because they combine the advantages of each subelement [1–3]. Typical hybrid systems include atoms coupled to photons [4], optomechanical systems [5], cavity magnonics systems [6], superconducting qubits coupled to spins [3], and so on. Among them, a hybrid quantum system involving the coherent coupling between a transmon qubit and a magnon has received widespread attention and been considered as a promising architecture for quantum information processing [7]. Specifically, in such a hybrid system, the transmon qubit serves as a quantum information processor [8], while the magnon functions as a quantum memory due to its long coherence time [6]. Recently, based on the entanglement between the transmon qubit and the magnon, the detection of a single magnon with a quantum efficiency of up to 0.71 has been demonstrated by using a transmon qubit as a quantum sensor [9]. The magnon blockade in a hybrid ferromagnet-superconductor quantum system has been studied [10]. The generation of nonclassical quantum states in a transmon-magnon system has also been reported [11–13].

The magnon has a high spin density, which exceeds previous spin ensembles by several orders of magnitude [14–16]. It can be ultrastrongly coupled to a cavity, which forms the setup of the cavity magnonics systems [6] and plays an important role in exploring quantum information science [17,18]. Non-Hermitian physics [19,20], the magnon Kerr effect [21], quantum entanglement generation [22–30], the bistability phenomenon [31], quantum phase transitions [32,33], nonreciprocity [34,35], magnon blockades [36,37], and magnon-assisted photon-phonon conversion [38] have been demonstrated in cavity magnonics systems.

On the other hand, among various types of superconducting qubits, a transmon qubit is considered as one of the most promising candidates for building up quantum processors due to its small wiring overhead [39]. The transmon qubit consists of two main parts: One is the Josephson junction and the other is the shunt capacitor [39]. The Josephson junction is a nonlinear circuit element, which plays a crucial role in the realization of quantum information processing and quantum computing [40,41]. The transmon is an artificial system, with advantages in controllability, compatibility, and integrability [39]. It can strongly and controllably interact with microwave photons [41]. The anharmonicity of the energy spectrum of the transmon is robust against charge-type $1/f$ noises. Based on the transmon platform, the quantum supremacy of a 53-qubit system [42] and a two-dimensional programmable quantum processor (*Zuchongzhi*) [8] have been demonstrated.

In this paper, we describe a method that enables a tunable and strong coupling between a magnon and a transmon. Different from the coupling of a magnon and a transmon via the virtual photon excitation of a microwave cavity [7,11], the transmon in this work is coupled to cavity c_1 and the magnon is coupled to cavity c_2. The two cavities c_1 and c_2 are coupled via a hopping interaction. The coupling strength between the transmon and the cavity c_1 can be adjusted by an external magnetic flux [39]. The coupling strength between the magnon and the cavity c_2 can be controlled by changing the position of the magnon in the cavity [19]. The high-fidelity quantum information transfer from the transmon to the magnon, the maximally entangled state between the

*dllgzfy@126.com
†yangcp@hznu.edu.cn

FIG. 1. Schematic of the coherent coupling system. A transmon is capacitively coupled to microwave cavity c_1, while a magnon is coupled to microwave cavity c_2 via the magnetic dipole interaction. The two microwave cavities c_1 and c_2 are coupled via a hopping interaction. Each cavity can be a one-dimensional or three-dimensional cavity.

transmon and the magnon, and the W-type state of transmons are demonstrated. The transmon is considered as an information processor, while the magnon acts as an information memorizer. Therefore, we can construct a quantum information processor, which has integrated the advantages in easy controllability and long coherence time. This model has potential applications in realizing a hybrid solid quantum information processor module.

II. MODEL AND HAMILTONIAN

The model is shown in Fig. 1. A transmon is capacitively coupled to microwave cavity c_1, while a magnon is coupled to microwave cavity c_2 via the magnetic dipole interaction. The two microwave cavities c_1 and c_2 are coupled via a hopping interaction. Each cavity can be a one-dimensional or three-dimensional cavity.

The transmon is considered as one kind of superconducting qubits. The Hamiltonian of the transmon can be quantized by introducing the canonical variables. The canonical variables in the transmon are the charge number operator $\hat{n}$ and the phase operator $\hat{\varphi}$, which satisfy the commutation relationship $[\hat{\varphi}, \hat{n}] = i$. The Hamiltonian of the transmon can be written as $H_q = 4E_C\hat{n}^2 + \frac{1}{2}E_J\hat{\varphi}^2$ with the charge energy E_C and the Josephson energy E_J [39,41]. The transmon can be equivalent to an ideal two-level system. Then, the Hamiltonian of the transmon is mapped to a spin-1/2 fermionic system (setting $\hbar = 1$) $H_q = \frac{\omega_q}{2}\sigma_z$, where $\omega_q = \sqrt{8E_CE_J} - E_C$ is the transition frequency between the ground and first excited states, and $\sigma_z = |e\rangle\langle e| - |g\rangle\langle g|$ is the Pauli z operator [39,41]. Here, $|g\rangle$ and $|e\rangle$ are the ground and excited states of the transmon, respectively. The transmon can naturally be capacitively coupled to a microwave cavity. The combined system can be described by a well-known Jaynes-Cummings Hamiltonian. Under the rotating-wave approximation, the interaction Hamiltonian between the microwave cavity c_1 and the transmon is $H_{I,q} = g_q(c_1\sigma_+ + c_1^\dagger\sigma_-)$, where c_1 ($c_1^\dagger$) is the annihilation (creation) operator of the microwave cavity c_1, $\sigma_+ = |e\rangle\langle g|$ ($\sigma_- = |g\rangle\langle e|$) is the rising (lowering) operator of the transmon, and $g_q = \omega_a\frac{C_g}{C_\Sigma}(\frac{E_J}{2E_C})^{1/4}\sqrt{\frac{\pi Z_r}{R_k}}$ is the coupling strength. Here, the parameter ω_a is the frequency of microwave cavity c_1, C_g is the gate capacitance, $C_\Sigma = C_S + C_J$ is the total capacitance with the shunt capacitance C_S and the junction capacitance C_J, Z_r is the characteristic impedance of the cavity mode, and R_k is the resistance quantum.

The magnon is the collective excitation of a large number of spins [14,15]. The collective spin can be described by a bosonic creation operator $m^\dagger$ and an annihilation operator m [21,43]. Thus, the free Hamiltonian of the magnon is given by $H_m = \omega_m m^\dagger m$. Here, $\omega_m = \bar{\gamma}H_0$ is the frequency of the magnon mode which can be adjusted by varying the bias magnetic field H_0, and $\bar{\gamma}/2\pi = 28$ GHz/T is the gyromagnetic ratio for the yttrium iron garnet (YIG). Under the rotating-wave approximation, the interaction Hamiltonian between the magnon and the microwave cavity c_2 is $H_{I,m} = g_m(mc_2^\dagger + m^\dagger c_2)$ [44], where $c_2^\dagger$ (c_2) is the creation (annihilation) operator of the cavity c_2, and $g_m = \eta\gamma\sqrt{\omega_b\mu_0\mathcal{N}s/2V}$ is the coupling strength. Here, η describes the spatial overlap and polarization matching conditions between the microwave field and the magnon, ω_b is the cavity frequency, V is the mode volume of the microwave cavity, $\mathcal{N}$ is the total number of spins, and s is the spin number of the ground state.

The full Hamiltonian of the total system is

$$H = H_q + H_m + H_c + H_{I,q} + H_{I,m}, \tag{1}$$

where $H_q = \frac{\omega_q}{2}\sigma_z$ is the free Hamiltonian of the transmon, $H_m = \omega_m m^\dagger m$ is the free Hamiltonian of the magnon, $H_{I,q} = g_q(c_1\sigma_+ + c_1^\dagger\sigma_-)$ is the interaction Hamiltonian between the microwave cavity c_1 and the transmon, $H_{I,m} = g_m(mc_2^\dagger + m^\dagger c_2)$ is the interaction Hamiltonian between the magnon and the microwave cavity c_2, and $H_c = \omega_a c_1^\dagger c_1 + \omega_b c_2^\dagger c_2 + \lambda(c_1^\dagger c_2 + c_2^\dagger c_1)$ is the Hamiltonian of the coupled cavities with coupling strength λ. Coupled cavities have the advantage of easily addressing individual sites with a control field. This structure can be applied to realize a data bus between the two subsystems. By introducing the normal coordinates $a = \frac{1}{\sqrt{2}}(c_1 - c_2)$ and $b = \frac{1}{\sqrt{2}}(c_1 + c_2)$, the Hamiltonian of the coupled cavities can be diagonalized as $H_c = \lambda_1 a^\dagger a + \lambda_2 b^\dagger b$ (setting $\omega_a = \omega_b = \omega_c$) with $\lambda_1 = \omega_c - \lambda$ and $\lambda_2 = \omega_c + \lambda$.

In the interaction picture, the Hamiltonian of the coherent coupling between the magnon and the transmon is given by

$$\begin{aligned} H_I = \frac{1}{\sqrt{2}}[&g_q\sigma_+ a e^{-i\delta_1 t} + g_q\sigma_- a^\dagger e^{i\delta_1 t} \\ &+ g_q\sigma_+ b e^{-i\delta_2 t} + g_q\sigma_- b^\dagger e^{i\delta_2 t} \\ &- g_m m^\dagger a e^{-i\nu_1 t} - g_m m a^\dagger e^{i\nu_1 t} \\ &+ g_m m^\dagger b e^{-i\nu_2 t} + g_m m b^\dagger e^{i\nu_2 t}], \end{aligned} \tag{2}$$

where $\delta_k = \lambda_k - \omega_q$ and $\nu_k = \lambda_k - \omega_m$ with $k = \{1, 2\}$. Under the large detuning conditions $g_q \ll \delta_k$ and $g_m \ll \nu_k$, and assuming that the normal modes are in the vacuum state, we can obtain the following effective Hamiltonian [45,46]:

$$\begin{aligned} H_e = \frac{1}{2}\Bigg[&-g_q^2\left(\frac{1}{\delta_1} + \frac{1}{\delta_2}\right)\sigma_+\sigma_- - g_m^2\left(\frac{1}{\nu_1} + \frac{1}{\nu_2}\right)m^\dagger m \\ &+ g_q g_m\left(\frac{1}{\nu_1}e^{-i(\delta_1-\nu_1)t} - \frac{1}{\nu_2}e^{-i(\delta_2-\nu_2)t}\right)\sigma_+ m \\ &+ g_q g_m\left(\frac{1}{\delta_1}e^{i(\delta_1-\nu_1)t} - \frac{1}{\delta_2}e^{i(\delta_2-\nu_2)t}\right)m^\dagger\sigma_-\Bigg]. \end{aligned} \tag{3}$$

By performing an unitary transformation $U = \exp(-iH_0 t)$ with $H_0 = \frac{1}{2}[-g_q^2(\frac{1}{\delta_1} + \frac{1}{\delta_2})\sigma_+\sigma_- - g_m^2(\frac{1}{\nu_1} + \frac{1}{\nu_2})m^\dagger m]$ and applying the conditions $\delta_1 = \nu_1$, $\delta_2 = \nu_2$, and $g_q = g_m = g$, the effective Hamiltonian (3) becomes

$$H_e = J(\sigma_- m^\dagger + m\sigma_+), \tag{4}$$

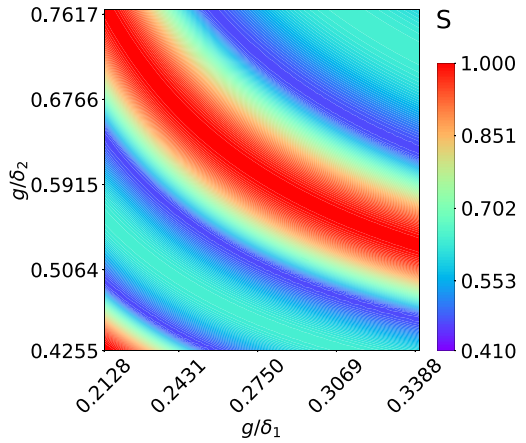

FIG. 2. The synchronization between the full Hamiltonian and the effective Hamiltonian vs the parameters g/δ_1 and g/δ_2.

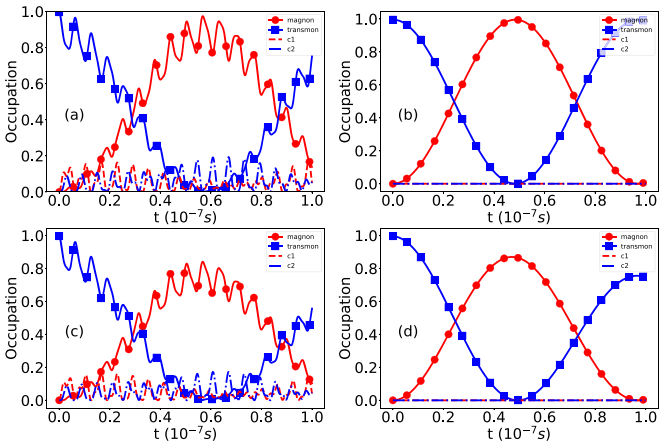

FIG. 3. The occupation numbers of the system vs the evolution: (a) and (c) correspond to the full Hamiltonian; (b) and (d) correspond to the effective Hamiltonian. In (a) and (b) the parameter values are $\kappa_m = \kappa_q = \kappa_{c_i} = 0$. In (c) and (d) the parameter values are $\kappa_q/2\pi = 0.13$ MHz, $\kappa_m/2\pi = 0.775$ MHz, and $\kappa_{c_i}/2\pi = 0.1$ MHz. The other parameter values can be found in the main text.

where the parameter $J = \frac{g^2}{2}(\frac{1}{\delta_1} - \frac{1}{\delta_2})$ is the effective coupling strength between the magnon and the transmon. The effective coupling strength J depends on the parameters g, δ_1, and δ_2. Therefore, the transmon-magnon effective coupling strength can be adjusted by changing the parameters g, δ_1, and δ_2. Figure 2 shows the synchronization between the complete Hamiltonian and the effective Hamiltonian with the parameters g/δ_1 and g/δ_2. The detunings δ_1 and δ_2 can be changed by adjusting the frequencies ω_q and ω_m. The magnon's frequency ω_m can be tuned by adjusting the bias magnetic field. The transmon's frequency ω_q can be controlled by the external parameters. Considering the feasibility of the current experimental conditions, the parameter values of the coplanar cavity are used to simulate the results. To evaluate the transmon-magnon coupling strength J, we choose experimentally feasible parameters as follows: The hopping coupled strength $\lambda/2\pi = 90$ MHz for the two neighboring coplanar cavities c_1 and c_2 [47], the transmon's bare frequency $\omega_q/2\pi = 8.204$ GHz [7], the damping rate of the transmon $\kappa_q/2\pi = 0.13$ MHz [7] (0.38 MHz [48]), the frequency of the coplanar cavity $\omega_c/2\pi = 9.3$ GHz [49], the damping rate of the coplanar cavity $\kappa_c/2\pi = 0.1$ MHz [50], and the damping rate of the magnon $\kappa_m/2\pi = 1$ MHz [17] (0.775 MHz [51]). Here, we choose the frequency of the coplanar cavity $\omega_c/2\pi = 8.420$ GHz. The frequency of the magnon ranges from several hundreds of MHz to 28 GHz [21]. Thus, we choose the frequency of the magnon $\omega_m/2\pi = 8.204$ GHz. The coupling strength between the magnon and the coplanar cavity can reach up to $g_m/2\pi = 450$ MHz [49]. The coupling strength between the coplanar cavity and the transmon can reach up to $g_q/2\pi = 897$ MHz [52]. Here, we choose the coupling strength $g_q/2\pi = g_m/2\pi = 47$ MHz. Based on the above parameter values, the effective coupling strength between the transmon and the magnon is $J/2\pi = 5.16$ MHz. We choose the damping rate of the magnon $\kappa_m/2\pi = 1$ MHz and the damping rate of the transmon $\kappa_q/2\pi = 1$ MHz. A dimensionless measure of the coupling strength of a hybrid system is the cooperativity [53,54] $C = J^2/\kappa_m\kappa_q \approx 26.6$. The cooperativity value representing this system is in the strong-coupling regime [50].

When the dissipation of the system is considered, the full dynamics of the system is described by the master equation

$$\dot{\rho} = -i[H, \rho] + \kappa_m\mathcal{D}[m]\rho + \kappa_q\mathcal{D}[\sigma_-]\rho + \kappa_{c_1}\mathcal{D}[c_1]\rho + \kappa_{c_2}\mathcal{D}[c_2]\rho, \quad (5)$$

where H is the full Hamiltonian (1); ρ is the density matrix of the system; the standard Lindblad superoperator $\mathcal{D}[o]\rho = o\rho o^\dagger - \frac{1}{2}o^\dagger o\rho - \frac{1}{2}\rho o^\dagger o$ represents the decoherence term for a given operator o; κ_{c_1} and κ_{c_2} are the damping rates of the cavity modes c_1 and c_2, respectively. In Fig. 3, we show the time evolutions of the system through solving the master equation (5). The population can be transferred from the transmon to the magnon even if the dissipation of the system is considered, and vice versa. Meanwhile, we have verified that the large detuning conditions are satisfied. The full Hamiltonian and the effective Hamiltonian approximately lead to the same dynamical evolution.

III. APPLICATIONS IN THE QUANTUM INFORMATION PROCESSOR

We only consider the single excitation of the system. The excited subspaces of the transmon and the magnon are formed by $\{|0\rangle_q, |1\rangle_q\}$ and $\{|0\rangle_m, |1\rangle_m\}$, respectively. Here, $|0\rangle_m(|0\rangle_q)$ and $|1\rangle_m(|1\rangle_q)$ are the ground and excited states of the magnon (transmon). The corresponding time evolution operator for the Hamiltonian (4) reads

$$U(t) = \begin{pmatrix} 1 & 0 & 0 & 0 \\ 0 & \cos(Jt) & -i\sin(Jt) & 0 \\ 0 & -i\sin(Jt) & \cos(Jt) & 0 \\ 0 & 0 & 0 & 1 \end{pmatrix}. \quad (6)$$

For $Jt = \pi/2$, the unitary operator $U(t)$ leads to the following state transformation,

$$U(t)|0\rangle_q|0\rangle_m \to |0\rangle_q|0\rangle_m, \quad U(t)|0\rangle_q|1\rangle_m \to -i|1\rangle_q|0\rangle_m,$$
$$U(t)|1\rangle_q|0\rangle_m \to -i|0\rangle_q|1\rangle_m, \quad U(t)|1\rangle_q|1\rangle_m \to |1\rangle_q|1\rangle_m, \quad (7)$$

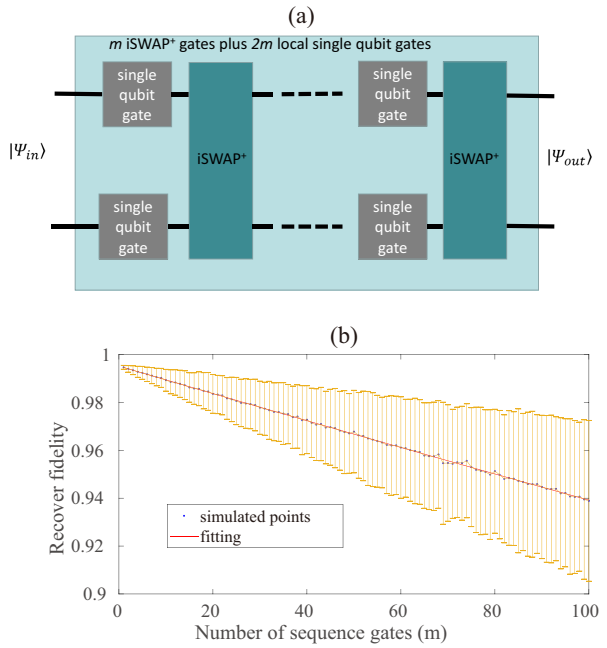

FIG. 4. (a) The circuit used in the randomized benchmarking of the iSWAP† gate. (b) The average fidelity obtained in the randomized benchmarking as a function of the number of gates.

which shows a two-qubit iSWAP† gate. When the evolution time takes $t = \pi/2J \approx 0.048$ μs, the information transfer from the transmon to the magnon can be realized.

How to characterize the fidelity of logic gates is very important. The standard method for characterizing a logic gate is quantum process tomography [55]. This method has two disadvantages: (i) It is unscalable; and (ii) the errors caused by measurement and state preparation will affect the characterization of the logic gate [56]. Here, we use the randomized benchmarking (RB) method to estimate the average fidelity of the iSWAP† gate. The general thought of RB is as follows: We apply a random sequence of quantum gates that compose to the identity operation, and measure the fidelity of each sequence [57,58]. The RB method has been used to characterize the gate fidelity [57–62]. Figure 4(a) presents the circuit diagram of the RB is consisting of m iSWAP† gates and $2m$ local single-qubit gates [62]. The random local single-qubit gate is written as [62]

$$L_j(\mu_j, \nu_j, \lambda_j) = \begin{pmatrix} \cos(\mu_j/2), & -e^{i\lambda_j}\sin(\mu_j/2) \\ e^{i\nu_j}\sin(\mu_j/2), & e^{i(\lambda_j+\nu_j)}\cos(\mu_j/2) \end{pmatrix}, \tag{8}$$

with $\mu_j \subseteq [0, 2\pi]$ and $\nu_j(\lambda_j) \subseteq [0, \pi]$. For pure states, the fidelity of a single realization is $F = |\langle\Psi_{\text{ideal}}|\Psi_{\text{error}}\rangle|^2$, where $|\Psi_{\text{ideal}}\rangle$ is the ideal state while $|\Psi_{\text{error}}\rangle$ is the simulation state with dissipation. Through averaging the circuit over 1000 realizations, Fig. 4(b) shows the result with up to 100 iSWAP† gates plus 100 pairs of local qubit gates. According to the fit $F(m) = \bar{F}^m$, one gets the average fidelity $\bar{F} = 0.9993$ by fitting the set of data.

For the initial state $|\Psi_i\rangle = (\cos\theta|0\rangle_q + \sin\theta|1\rangle_q)|0\rangle_m$, the fidelity of the iSWAP† gate is defined as $F_1 = \frac{1}{2\pi}\int_0^{2\pi}\langle\Psi_f|\varrho|\Psi_f\rangle d\theta$, where $|\Psi_f\rangle = U(\pi/2J)|\Psi_i\rangle$ is the ideal final state and ϱ is a reduced density matrix. In Fig. 5, we present the fidelity through numerical simulations when the dissipation of the system is considered.

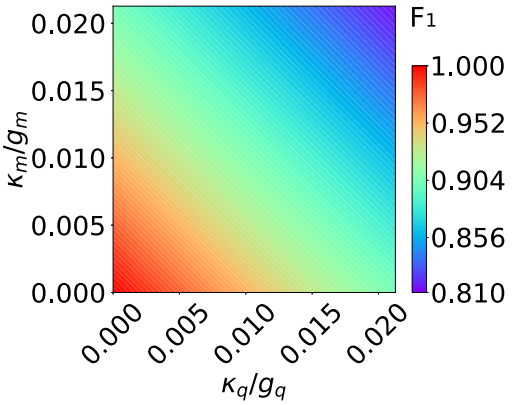

FIG. 5. The fidelity vs the dimensionless parameters κ_m/g_m and κ_q/g_q.

In addition, this system can be used to generate the entanglement between the transmon and the magnon. Initially, we assume that the transmon is prepared in the excited state $|1\rangle_q$, and the magnon is prepared in the ground state $|0\rangle_m$. So, the initial state of the system is $|\Psi(0)\rangle = |1\rangle_q|0\rangle_m$. Under the Hamiltonian (4), the initial state evolves to $|\Psi(\tau)\rangle = (|1\rangle_q|0\rangle_m - i|0\rangle_q|1\rangle_m)/\sqrt{2}$ with an evolution time $\tau = \pi/4J$. Thus, the maximally entangled state is generated between the transmon and the magnon. We can evaluate the time of generating the maximally entangled state $\tau = \pi/4J \approx 0.024$ μs, which is much smaller than the relaxation time of the transmon (0.5 ms [63]) and the memory time of the magnon (5.11 s [64]). When the dissipation of the system is considered, the fidelity is $F_2 = \langle\Psi(\tau)|\varrho|\Psi(\tau)\rangle$. From Fig. 6, we can see that the high-fidelity entangled state is obtained even if the decay of the system is taken into account.

Our proposal can be extended to a magnon coupled to multiple transmons, as shown in Fig. 7. For a magnon coupled to multiple transmons, we can control the interaction between any selected transmon and the magnon. So, the information

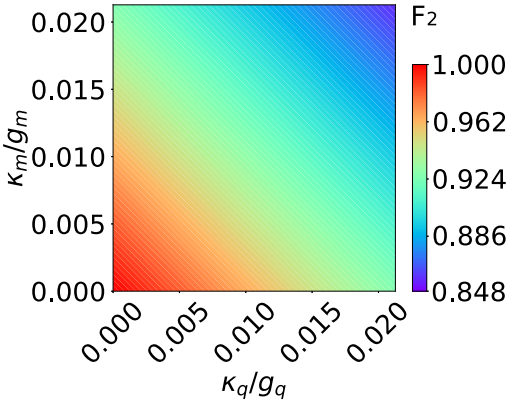

FIG. 6. The fidelity vs the dimensionless parameters κ_m/g_m and κ_q/g_q.

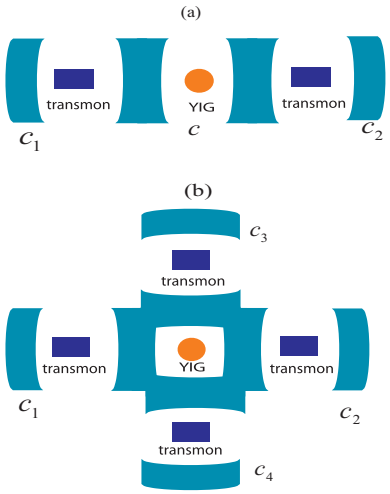

FIG. 7. Schematic of the coherent coupling system. (a) One-dimensional model of 3 lattice sites. (b) Two-dimensional model of five lattice sites.

of each transmon can be transferred to the magnon one by one. The time of achieving the information transfer from a transmon to a magnon is $t = 0.048$ μs, which is much shorter than the relaxation time of the transmon and the memory time of the magnon. Therefore, we can achieve information transfer thousands of times before the decoherence of the system occurs. Also, the entanglement between any selected transmon and the magnon can be generated by controlling their coupling.

One of the favorable applications for this system is to generate multiqubit entangled states of transmons. The multiqubit entangled states have attracted much interest because of their potential applications in quantum information processing and quantum communication. The W-type state [65] is one class of multiqubit entangled state, which is robust against loss of a qubit if we trace out any one qubit. Therefore, the W-type state can be used as an important resource for quantum information processing and quantum communication [66,67]. The procedure of generating a multiqubit entangled state of transmons is described as follows: We consider many transmons coupling to a common magnon simultaneously. The effective Hamiltonian of this system reads $H_M = \sum_i^N J_i(\sigma_-^i m^\dagger + m\sigma_+^i)$, where N is the number of transmons. For simplicity, we assume that each transmon is equally coupled to the magnon, that is, $J_i = J$. If the system is initially prepared in the state $|\Psi(0)\rangle = |1\rangle_{q1}|1\rangle_{q2}\cdots|1\rangle_{qN}|0\rangle_m$, the state evolution under the Hamiltonian H_M is given by $|\Psi(t)\rangle = \cos(\sqrt{N}Jt)|1\rangle_{q1}|1\rangle_{q2}\cdots|1\rangle_{qN}|0\rangle_m + (1/\sqrt{N})\sin(\sqrt{N}Jt)\sum_i^N |1\rangle_{q1}\cdots|0\rangle_{qi}\cdots|1\rangle_{qN}|1\rangle_m$. The W-type state $|\Psi_W\rangle = (1/\sqrt{N})\sum_i^N |1\rangle_{q1}\cdots|0\rangle_{qi}\cdots|1\rangle_{qN}$ of transmons can be obtained by controlling the evolution time as $t = \pi/2\sqrt{N}J$ and measuring the quantum state of the magnon which collapses in the state $|1\rangle_m$.

IV. DISCUSSIONS AND CONCLUSIONS

We now consider the experimental feasibility of the coherent coupling between the magnon and the transmon. In this paper, the coupling system mainly includes three kinds of different coupling mechanisms: The transmon is capacitively coupled to a microwave cavity, the magnon is magnetically coupled to the other microwave cavity, and the two microwave cavities are coupled via a hopping interaction. With the improvement of the current experimental condition, the coupling technology between a transmon and a microwave cavity is rather mature, where five-transmon [59] and ten-transmon [68] qubits coupling with a cavity have been realized. Recently, the experimental platform of the cavity magnonics system has demonstrated important scientific breakthroughs. The coherent coupling between two magnons and a microwave cavity has been demonstrated [64]. A one-dimensional chain of 72 lattice sites has been implemented [47]. Each site comprises a coplanar waveguide cavity coupled to a transmon qubit [47]. The coupling between the coplanar microwave cavity and the magnon [49], and the coupling between the coplanar microwave cavity and the transmon [52], have been realized. So, our model can be built with current experimental technology.

In summary, we have proposed a method to realize the tunable coupling between a transmon and a magnon. Through calculating the cooperativity, we have found this hybrid system can work in the strong-coupling regime. In addition, we have demonstrated applications of this system to quantum information. The high-fidelity realization of an $i\text{SWAP}^\dagger$ gate and the generation of a maximally entangled state with this coupling system have been realized even if the dissipation of the system is considered. Such a hybrid quantum system can be used to generate the entanglement between any selected transmon and a magnon, and can also be used to create multiqubit W states of transmons.

ACKNOWLEDGMENTS

We acknowledge Tao Xin and Bao Liu for valuable discussions. The authors gratefully acknowledge the use of the open source PYTHON numerical packages QUTIP [69,70]. This work was partially supported by the National Natural Science Foundation of China under Grants No. U21A20436, No. 11505024, No. 12364048, No. 12264040, No. 11074062, No. 11374083, and No. 11774076. This work was also supported by Innovation Program for Quantum Science and Technology (Grant No. 2021ZD0301705), the Jiangxi Natural Science Foundation under Grants No. 20232BCJ23022, No. 20212BAB211019, and No. 20212BAB211018, and the Fundamental Research Funds for the Central Universities.

[1] Z. L. Xiang, S. Ashhab, J. Q. You, and F. Nori, Hybrid quantum circuits: Superconducting circuits interacting with other quantum systems, Rev. Mod. Phys. **85**, 623 (2013).

[2] G. Kurizki, P. Bertet, Y. Kubo, K. Mølmer, D. Petrosyan, P. Rabl, and J. Schmiedmayer, Quantum technologies with hybrid systems, Proc. Natl. Acad. Sci. USA **112**, 3866 (2015).

[3] A. A. Clerk, K. W. Lehnert, P. Bertet, J. R. Petta, and Y. Nakamura, Hybrid quantum systems with circuit quantum electrodynamics, Nat. Phys. **16**, 257 (2020).

[4] S. Haroche and J. M. Raimond, *Exploring the Quantum* (Oxford University Press, Oxford, UK, 2006).

[5] M. Aspelmeyer, T. J. Kippenberg, and F. Marquardt, Cavity optomechanics, Rev. Mod. Phys. **86**, 1391 (2014).

[6] B. Z. Rameshti, S. V. Kusminskiy, J. A. Haigh, K. Usami, D. Lachance-Quirion, Y. Nakamura, C. M. Hu, H. X. Tang, G. E. W. Bauer, and Y. M. Blanter, Cavity magnonics, Phys. Rep. **979**, 1 (2022).

[7] Y. Tabuchi, S. Ishino, A. Noguchi, T. Ishikawa, R. Yamazaki, K. Usami, and Y. Nakamura, Coherent coupling between a ferromagnetic magnon and a superconducting qubit, Science **349**, 405 (2015).

[8] Y. Wu, W. S. Bao, S. Cao F. Chen, M.-C. Chen, X. Chen, T.-H. Chung, H. Deng, Y. Du, D. Fan *et al.*, Strong quantum computational advantage using a superconducting quantum processor, Phys. Rev. Lett. **127**, 180501 (2021).

[9] D. Lachance-Quirion, S. P. Wolski, Y. Tabuchi, S. Kono, K. Usami, and Y. Nakamura, Entanglement-based single-shot detection of a single magnon with a superconducting qubit, Science **367**, 425 (2020).

[10] Z. X. Liu, H. Xiong, and Y. Wu, Magnon blockade in a hybrid ferromagnet-superconductor quantum system, Phys. Rev. B **100**, 134421 (2019).

[11] D. Xu, X. K. Gu, H. K. Li, Y. C. Weng, Y. P. Wang, J. Li, H. Wang, S. Y. Zhu, and J. Q. You, Quantum control of a single magnon in a macroscopic spin system, Phys. Rev. Lett. **130**, 193603 (2023).

[12] S. He, X. Xin, F. Y. Zhang, and C. Li, Generation of a Schrödinger cat state in a hybrid ferromagnet-superconductor system, Phys. Rev. A **107**, 023709 (2023).

[13] Q. Guo, J. Cheng, H. Tan, and J. Li, Magnon squeezing by two-tone driving of a qubit in cavity-magnon-qubit systems, Phys. Rev. A **108**, 063703 (2023).

[14] Ö. O. Soykal and M. E. Flatté, Strong field interactions between a nanomagnet and a photonic cavity, Phys. Rev. Lett. **104**, 077202 (2010).

[15] Ö. O. Soykal and M. E. Flatté, Size dependence of strong coupling between nanomagnets and photonic cavities, Phys. Rev. B **82**, 104413 (2010).

[16] X. Zhang, C.-L. Zou, L. Jiang, and H. X. Tang, Strongly coupled magnons and cavity microwave photons, Phys. Rev. Lett. **113**, 156401 (2014).

[17] D. Lachance-Quirion, Y. Tabuchi, A. Gloppe, K. Usami, and Y. Nakamura, Hybrid quantum systems based on magnonics, Appl. Phys. Express **12**, 070101 (2019).

[18] H. Y. Yuan, Y. Cao, A. Kamra, R. A. Duine, and P. Yan, Quantum magnonics: When magnon spintronics meets quantum information science, Phys. Rep. **965**, 1 (2022).

[19] D. Zhang, X. Q. Luo, Y. P. Wang, T. F. Li, and J. Q. You, Observation of the exceptional point in cavity magnon-polaritons, Nat. Commun. **8**, 1368 (2017).

[20] F. Y. Zhang, Q. C. Wu, and C. P. Yang, Non-Hermitian shortcut to adiabaticity in Floquet cavity electromagnonics, Phys. Rev. A **106**, 012609 (2022).

[21] Y. P. Wang, G. Q. Zhang, D. K. Zhang, X. Q. Luo, W. Xiong, S. P. Wang, T. F. Li, C. M. Hu, and J. Q. You, Magnon Kerr effect in a strongly coupled cavity-magnon system, Phys. Rev. B **94**, 224410 (2016).

[22] J. Li, S. Y. Zhu, and G. S. Agarwal, Magnon-photon-phonon entanglement in cavity magnomechanics, Phys. Rev. Lett. **121**, 203601 (2018).

[23] H. Y. Yuan, P. Yan, S. Zheng, Q. Y. He, K. Xia, and M. H. Yung, Steady Bell state generation via magnon-photon coupling, Phys. Rev. Lett. **124**, 053602 (2020).

[24] J. Li and S. Y. Zhu, Entangling two magnon modes via magnetostrictive interaction, New J. Phys. **21**, 085001 (2019).

[25] M. Yu, H. Shen, and J. Li, Magnetostrictively induced stationary entanglement between two microwave fields, Phys. Rev. Lett. **124**, 213604 (2020).

[26] J. M. P. Nair and G. S. Agarwal, Deterministic quantum entanglement between macroscopic ferrite samples, Appl. Phys. Lett. **117**, 084001 (2020).

[27] J. Li and S. Gröblacher, Entangling the vibrational modes of two massive ferromagnetic spheres using cavity magnomechanics, Quantum Sci. Technol. **6**, 024005 (2021).

[28] S. S. Zheng, F. X. Sun, H. Y. Yuan, Z. Ficek, Q. H. Gong, and Q. Y. He, Enhanced entanglement and asymmetric EPR steering between magnons, Sci. China. Phys. Mech. Astron. **64**, 210311 (2021).

[29] H. Tan and J. Li, Einstein-Podolsky-Rosen entanglement and asymmetric steering between distant macroscopic mechanical and magnonic systems, Phys. Rev. Res. **3**, 013192 (2021).

[30] W. J. Wu, Y. P. Wang, J. Z. Wu, J. Li, and J. Q. You, Remote magnon entanglement between two massive ferrimagnetic spheres via cavity optomagnonics, Phys. Rev. A **104**, 023711 (2021).

[31] Y. P. Wang, G. Q. Zhang, D. Zhang, T. F. Li, C. M. Hu, and J. Q. You, Bistability of cavity magnon polaritons, Phys. Rev. Lett. **120**, 057202 (2018).

[32] J. Zhao, Y. Liu, L. Wu, C. K. Duan, Y. X. Liu, and J. Du, Observation of anti-$\mathcal{PT}$-symmetry phase transition in the magnon-cavity-magnon coupled system, Phys. Rev. Appl. **13**, 014053 (2020).

[33] G. Q. Zhang, Z. Chen, W. Xiong, C. H. Lam, and J. Q. You, Parity-symmetry-breaking quantum phase transition via parametric drive in a cavity magnonic system, Phys. Rev. B **104**, 064423 (2021).

[34] Y. P. Wang, J. W. Rao, Y. Yang, P. C. Xu, Y. S. Gui, B. M. Yao, J. Q. You, and C. M. Hu, Nonreciprocity and unidirectional invisibility in cavity magnonics, Phys. Rev. Lett. **123**, 127202 (2019).

[35] Y. Xu, J. Y. Liu, W. Liu, and Y. F. Xiao, Nonreciprocal phonon laser in a spinning microwave magnomechanical system, Phys. Rev. A **103**, 053501 (2021).

[36] J. K. Xie, S. L. Ma, and F. L. Li, Quantum-interference-enhanced magnon blockade in an yttrium-iron-garnet sphere coupled to superconducting circuits, Phys. Rev. A **101**, 042331 (2020).

[37] C. S. Zhao, X. Li, S. L. Chao, R. Peng, C. Li, and L. Zhou, Simultaneous blockade of a photon, phonon, and magnon induced by a two-level atom, Phys. Rev. A **101**, 063838 (2020).

[38] S. F. Qi and J. Jing, Magnon-assisted photon-phonon conversion in the presence of structured environments, Phys. Rev. A **103**, 043704 (2021).

[39] J. Koch, T. M. Yu, J. Gambetta, A. A. Houck, D. I. Schuster, J. Majer, A. Blais, M. H. Devoret, S. M. Girvin, and R. J.

Schoelkopf, Charge-insensitive qubit design derived from the Cooper pair box, Phys. Rev. A **76**, 042319 (2007).

[40] J. Q. You and F. Nori, Atomic physics and quantum optics using superconducting circuits, Nature (London) **474**, 589 (2011).

[41] A. Blais, A. L. Grimsmo, S. M. Girvin, and A. Wallraff, Circuit quantum electrodynamics, Rev. Mod. Phys. **93**, 025005 (2021).

[42] F. Arute, K. Arya, R. Babbush, D. Bacon, J. C. Bardin, R. Barends, R. Biswas, S. Boixo, F. G. S. L. Brandao, D. A. Buell *et al.*, Quantum supremacy using a programmable superconducting processor, Nature (London) **574**, 505 (2019).

[43] H. Y. Yuan, S. Zheng, Z. Ficek, Q. Y. He, and M.-H. Yung, Enhancement of magnon-magnon entanglement inside a cavity, Phys. Rev. B **101**, 014419 (2020).

[44] X. Zhang, C. L. Zou, L. Jiang, and H. X. Tang, Cavity magnomechanics, Sci. Adv. **2**, e1501286 (2016).

[45] S. B. Zheng and G. C. Guo, Efficient scheme for two-atom entanglement and quantum information processing in cavity QED, Phys. Rev. Lett. **85**, 2392 (2000).

[46] D. F. James and J. Jerke, Effective Hamiltonian theory and its applications in quantum information, Can. J. Phys. **85**, 625 (2007).

[47] M. Fitzpatrick, N. M. Sundaresan, A. C. Y. Li, J. Koch, and A. A. Houck, Observation of a dissipative phase transition in a one-dimensional circuit QED lattice, Phys. Rev. X **7**, 011016 (2017).

[48] B. Kannan, M. J. Ruckriegel, D. L. Campbell, A. Frisk Kockum, J. Braumller, D. K. Kim, M. Kjaergaard, P. Krantz, A. Melville, B. M. Niedzielski *et al.*, Waveguide quantum electrodynamics with superconducting artificial giant atoms, Nature (London) **583**, 775 (2020).

[49] H. Huebl, C. W. Zollitsch, J. L. F. Hocke, M. Greifenstein, A. Marx, R. Gross, and S. T. B. Goennenwein, High cooperativity in coupled microwave resonator ferrimagnetic insulator hybrids, Phys. Rev. Lett. **111**, 127003 (2013).

[50] P. Forn-Díaz, L. Lamata, E. Rico, J. Kono, and E. Solano, Ultrastrong coupling regimes of light-matter interaction, Rev. Mod. Phys. **91**, 025005 (2019).

[51] R. C. Shen, J. Li, W. J. Wu, X. Zuo, Y. P. Wang, S. Y. Zhu, and J. Q. You, Observation of strong coupling between a mechanical oscillator and a cavity-magnon polariton, arXiv:2307.11328.

[52] S. J. Bosman, M. F. Gely, V. Singh, A. Bruno, D. Bothner, and G. A. Steele, Multi-mode ultra-strong coupling in circuit quantum electrodynamics, npj Quantum Inf. **3**, 46 (2017).

[53] D. I. Schuster, A. P. Sears, E. Ginossar, L. DiCarlo, L. Frunzio, J. J. L. Morton, H. Wu, G. A. D. Briggs, B. B. Buckley, D. D. Awschalom, and R. J. Schoelkopf, High-cooperativity coupling of electron-spin ensembles to superconducting cavities, Phys. Rev. Lett. **105**, 140501 (2010).

[54] Y. Kubo, F. R. Ong, P. Bertet, D. Vion, V. Jacques, D. Zheng, A. Dréau, J.-F. Roch, A. Auffeves, F. Jelezko, J. Wrachtrup, M. F. Barthe, P. Bergonzo, and D. Esteve, Strong coupling of a spin ensemble to a superconducting resonator, Phys. Rev. Lett. **105**, 140502 (2010).

[55] M. A. Nielsen and I. L. Chuang, *Quantum Computation and Quantum Information: 10th Anniversary Edition*, 10th ed. (Cambridge University Press, New York, 2011).

[56] E. Magesan, J. M. Gambetta, B. R. Johnson, C. A. Ryan, J. M. Chow, S. T. Merkel, M. P. da Silva, G. A. Keefe, M. B. Rothwell, T. A. Ohki, M. B. Ketchen, and M. Steffen, Efficient measurement of quantum gate error by interleaved randomized benchmarking, Phys. Rev. Lett. **109**, 080505 (2012).

[57] J. Emerson, R. Alicki, and K. Zyczkowski, Scalable noise estimation with random unitary operators, J. Opt. B: Quantum Semiclass. Opt. **7**, S347 (2005).

[58] E. Knill, D. Leibfried, R. Reichle, J. Britton, R. B. Blakestad, J. D. Jost, C. Langer, R. Ozeri, S. Seidelin, and D. J. Wineland, Randomized benchmarking of quantum gates, Phys. Rev. A **77**, 012307 (2008).

[59] R. Barends, J. Kelly, A. Megrant, A. Veitia, D. Sank, E. Jeffrey, T. C. White, J. Mutus, A. G. Fowler, B. Campbell *et al.*, Superconducting quantum circuits at the surface code threshold for fault tolerance, Nature (London) **508**, 500 (2014).

[60] T. Xin, S. Huang, S. Lu, K. Li, Z. Luo, Z. Yin, J. Li, D. Lu, G. Long, and B. Zeng, NMRCloudQ: a quantum cloud experience on a nuclear magnetic resonance quantum computer, Sci. Bull. **63**, 17 (2018).

[61] S. Li, B. J. Liu, Z. Ni, L. Zhang, Z. Y. Xue, J. Li, F. Yan, Y. Chen, S. Liu, M. H. Yung, Y. Xu, and D. Yu, Superrobust geometric control of a superconducting circuit, Phys. Rev. Appl. **16**, 064003 (2021).

[62] A. C. Santos, Role of parasitic interactions and microwave crosstalk in dispersive control of two superconducting artificial atoms, Phys. Rev. A **107**, 012602 (2023).

[63] C. Wang, X. Li, H. Xu, Z. Li, J. Wang, Z. Yang, Z. Mi, X. Liang, T. Su, C. Yang *et al.*, Towards practical quantum computers: transmon qubit with a lifetime approaching 0.5 milliseconds, npj Quantum Inf. **8**, 3 (2022).

[64] R. C. Shen, Y. P. Wang, J. Li, S. Y. Zhu, G. S. Agarwal, and J. Q. You, Long- time memory and ternary logic gate using a multistable cavity magnonic system, Phys. Rev. Lett. **127**, 183202 (2021).

[65] W. Dür, G. Vidal, and J. I. Cirac, Three qubits can be entangled in two inequivalent ways, Phys. Rev. A **62**, 062314 (2000).

[66] J. Joo, J. Lee, J. Jang, and Y. J. Park, Quantum secure communication with W States, arXiv:quant-ph/0204003.

[67] J. Joo, Y. J. Park, S. Oh, and J. Kim, Quantum teleportation via a W state, New J. Phys. **5**, 136 (2003).

[68] C. Song, K. Xu, W. Liu, C. P. Yang, S. B. Zheng, H. Deng, Q. Xie, K. Huang, Q. Guo, L. Zhang *et al.*, 10-Qubit entanglement and parallel logic operations with a superconducting circuit, Phys. Rev. Lett. **119**, 180511 (2017).

[69] J. Johansson, P. Nation, and F. Nori, QuTiP: An open-source Python framework for the dynamics of open quantum systems, Comput. Phys. Commun. **183**, 1760 (2012).

[70] J. Johansson, P. Nation, and F. Nori, QuTiP 2: A Python framework for the dynamics of open quantum systems, Comput. Phys. Commun. **184**, 1234 (2013).